1. Archer, A. W., Kuecher, G. J. and Kvale, E. P., The role of tidal velocity asymmetries in the deposition of silty tidal rhythmites (Carboniferous, Eastern Interior Coal Basin, USA). *J. Sediment. Res. A*, 1995, **65**, 408–416.
2. Kvale, E. P., Johnson, H. W., Sonett, C. P., Archer, A. W. and Zawistoski, A., Calculating lunar retreat rates using tidal rhythmites. *J. Sediment. Res.*, 1999, **69**, 1154–1168.
3. Coughenour, L. C., Archer, A. W. and Lacovara, J. K., Calculating Earth–Moon system parameters from sub-yearly tidal deposit records: an example from the carboniferous trade water formation. *Sediment. Geol.*, 2013, **295**, 67–76.
4. Berry, W. B. N. and Barker, R. M., Fossil bivalve shells indicate longer month and year in Cretaceous than present. *Nature*, 1968, **217**, 938–939.
5. Williams, G. E., Geological constraints on the Precambrian history of Earth's rotation and the Moon's orbit. *Rev. Geophys.*, 2000, **38**, 37–59.
6. Sonett, C. P., Kvale, E. P., Zakharian, A., Chan, M. A. and Demko, T. M., Late Proterozoic and Paleozoic tides, retreat of the Moon, and rotation of the Earth. *Science*, 1996, **273**, 100–104.
7. Archer, A. W. and Greb, S. W., Hyper tidal facies from the Pennsylvanian Period, Eastern and Western Interior Coal Basins, USA. In *Principles of Tidal Sedimentology* (eds Davis, R. A. and Dalrymple, R. W.), Springer, 2012.
8. Visser, R., Neap–spring cycles reflected in Holocene sub tidal large-scale bed form deposits: a preliminary note. *Geology*, 1980, **8**, 543–546.
9. Khosla, A. *et al.*, First dinosaur remains from the Cenomanian–Turonian Nimar Sandstone (Bagh Beds), District Dhār, Madhya Pradesh, India. *J. Paleontol. Soc. India*, 2003, **48**, 115–127.
10. Singh, S. K. and Srivastava, H. K., Lithostratigraphy of Bagh Beds and its correlation with Lameta Beds. *J. Paleontol. Soc. India*, 1981, **26**, 77–85.
11. Bose, P. K. and Das, N. G., A transgressive storm and fair weather wave dominated shelf sequence, Cretaceous Nimar Formation, Chakrud, Madhya Pradesh, India. *Sediment. Geol.*, 1986, **46**(1–2), 147–167.
12. Mazumder, R. and Arima, M., Tidal rhythmites and their implications. *Earth–Sci. Rev.*, 2005, **69**, 79–95.
13. Allen, J. R. L., Lower cretaceous tides revealed by cross-bedding with mud drapes. *Nature*, 1981, **289**, 579–581.
14. Terwindt, J. H. J., Origin and sequences of sedimentary structures in onshore mesotidal deposits of the North Sea. In *Holocene Marine Sedimentation in the North Sea Basin* (eds Nio, S. D., Shuttenhelm, R. T. E. and van Weering, Tj. C. E.), Special Publication No. 5, International Association of Sedimentologists, Blackwell Scientific Publications, Boston, 1981, pp. 4–26.
15. Bhattacharya, B., Bandyopadhyay, S., Mahapatra, S. and Banerjee, S., Record of tide wave influence on the coal-bearing Permian Barakar Formation. *Sediment. Geol.*, 2012, **267–268**, 25–35.
16. Bhattacharya, H. N. and Bhattacharya, B., A Permo-Carboniferous tide–storm interactive system, Talchir Formation, Raniganj Basin, India. *J. Asian Earth Sci.*, 2006, **27**, 303–311.
17. Greb, S. F. and Archer, A. W., Rhythmite sedimentation in a mixed tide and wave deposit: Hazel Patch Sandstone (Pennsylvanian) Eastern Kentucky Coalfield. *J. Sediment. Res. B*, 1995, **65**, 96–106.
18. Guenther, D. B., Krauss, L. M. and Demarque, P., Testing the constancy of the gravitational constant using helioseismology. *Astrophys. J.*, 1998, **498**, 871–876.

Natural base isolation system for earthquake protection

Srijit Bandyopadhyay[1], Aniruddha Sengupta[1,*] and G. R. Reddy[2]

[1]Department of Civil Engineering, Indian Institute of Technology, Kharagpur 721 302, India
[2]Structural and Seismic Engineering Section, Homi Bhaba National Institute, Mumbai 400 094, India

The performance of a well-designed layer of sand, geo-grid, geo-textiles and composites like layer of sand mixed with shredded tyre (rubber) as low-cost base isolators is studied in shake table tests in the laboratory. The building foundation is modelled by a 200 mm × 200 mm and 40 mm thick, rigid plexi-glass block. The block is placed in the middle of a 1 m × 1 m tank filled with sand. The selected base isolator is placed between the block and the sand foundation. Accelerometers are placed on top of the footing and foundation sand layer. The displacement of the footing is also measured by transducers. The whole set-up is mounted on the shake table and subjected to sinusoidal motion with varying amplitude and frequency. Sand is found to be effective only at very high amplitude ($>0.65\ g$) of motion. Among all the different materials tested, the performance of a composite consisting of sand and 50% shredded rubber tyre placed under the footing is found to be the most promising as a low-cost, effective base isolator.

To find an economical and feasible way of designing new structures or strengthening existing ones for protection from damages during an earthquake is one of the challenges in civil engineering. The conventional approach to seismic hazard mitigation is to design structures with adequate strength and ability to deform in a ductile manner. Over the past two decades, newer concepts of structural vibration control, including seismic isolation, installation of passive and active/semi-active devices[1–4] have been growing in acceptance. Traditionally, earthquake-resistant design of low- to medium-rise buildings is particularly important, as their fundamental frequencies of vibration are within the range where earthquake-induced force (acceleration) is the highest as found during the Mexico City Earthquake[5,6]. One possible means to reduce the degree of amplification is to make the building more flexible[7]. In low to medium-rise buildings, this necessary flexibility can be achieved by the use of base isolation techniques. The primary mechanism for the reduction of shaking level in a base isolation method is energy dissipation.

*For correspondence. (e-mail: sengupta@civil.iitkgp.ernet.in)

Rubber bearings offer the simplest method of base isolation and are in use for the past three decades[6]. Laminated rubber bearings, which are made by vulcanization bonding of sheets of rubber to thin steel reinforcing plates or lead plugs, are currently the most commonly adopted system owing to the fact that they are stiff in the vertical direction and flexible in the horizontal direction. There are several examples of using this strategy for earthquake-resistant construction in the US, Chile, Indonesia, New Zealand, Italy, China and Japan. However, these methods of base isolation are not so affordable in a country like India. Thus development of low-cost, natural base isolation system is necessary.

The concept of low-cost and effective earthquake protection techniques using natural materials like sand has been studied in the past[8–10]. The use of a synthetic liner consisting of an ultra molecular weight, polyethylene, non-woven geo-textile, placed in the foundation of a structure, was also found to be an effective way of reducing seismic ground motion[11,12]. Soil reinforced with rubber demonstrates an increase in energy dissipation capability[13]. The feasibility of using shredded rubber mixed with sand as a natural base isolator was also studied[14,15]. This communication presents results of experimental studies into the performance of a layer of sand, geo-grid, geo-textile and sand mixed with shredded rubber tyre as low-cost base isolation system.

The laboratory model tests were performed on a 1 m × 1 m shake table. The table is shaken sinusoidally in a uniaxial horizontal direction by a 2800 rpm and 7 HP DC motor. A slotted circular mild steel disc of 300 mm diameter and 20 mm thickness is bolted to another circular disc of the same size (used as a support to the slotted disc). The supported disc is connected to the shaft of a motor. A steel crank shaft 500 mm long and 20 mm in diameter is connected to the slotted disc by bolts. The other end of the crank shaft is connected to a reciprocating rod, 500 mm long and 20 mm in diameter. The amplitude of sinusoidal motion can be varied by changing the position of the crank shaft in the calibrated slot of the disc. The other end of the reciprocating rod is connected to the base plate of the shaking table. The reciprocating rod is kept in the horizontal position during the motion by a bracket support. The speed of the motor can be controlled from a panel board which essentially consists of an electrical variant. The shaking table has a maximum stroke length of 150 mm and a peak frequency of 50 Hz.

The laboratory model tests are performed inside a 1 m × 1 m × 0.5 m (length × width × height) rectangular test box made up of 12 mm thick Perspex glass sheets. The sides of the box are fixed rigidly with steel angles to prevent any movement. The model box is fixed to the base plate of the shaking table with bolts so that no relative movement can occur. This base plate is fitted with smooth wheels which slide in the horizontal direction on two parallel rails. The three sides of the box are covered

with 30 mm thick thermocol sheets to minimize the reflection of the waves at the boundary. Sand particles are glued to the bottom surface of the model box to generate surface roughness, so that there is no slippage along the bottom surface during shaking. The whole test set-up is shown in Figure 1.

In the laboratory model tests, a typical isolated building foundation or square footing is scaled down eight times (scale factor, $\lambda = 8$) geometrically and modelled by a 200 mm × 200 mm and 40 mm thick, rigid, plexi-glass block. The basic objective of the study is to find a low-cost yet effective base isolator for medium-storied buildings. For this reason, the transmissibility of the base isolator under the foundation is of major concern. Hence, the overall complex response of the structure, foundation and ground is not studied. The normal stress (normal load) on the foundation due to the super structure is imparted by a number of steel plates (weights) bolted on top of the plexi-glass block. A typical normal stress of 2 kPa has been considered here on top of the footing. This vertical load represents scaled column load coming from a typical four-storied residential building. A coarse sand paper is glued to the bottom side of the footing block to model the roughness of the footing. In the laboratory shake table tests, the test container is first filled with sand up to 200 mm height and compacted to a relative density of 65%. The mass density of the foundation soil is not scaled in this study. The model footing is then placed in the middle of the test box on top of the compacted sand foundation. The test box along with the sand foundation and the model footing are shaken by sinusoidal motions of given amplitude and frequency. Details of shake table arrangement are shown in Figure 1.

The acceleration responses during shaking are measured using accelerometers. Two accelerometers are mounted on the base plate of the shake table to measure the horizontal and vertical vibrations. The measurement in the vertical direction is made only to keep track of the vertical component of the motion, if any, generated by the table. Two other accelerometers are fixed on the walls of the test box. One accelerometer is placed at the foundation of the model footing and the other on top of the model footing. A sound and vibration meter is used for data acquisition. No scaling of the acceleration is done in
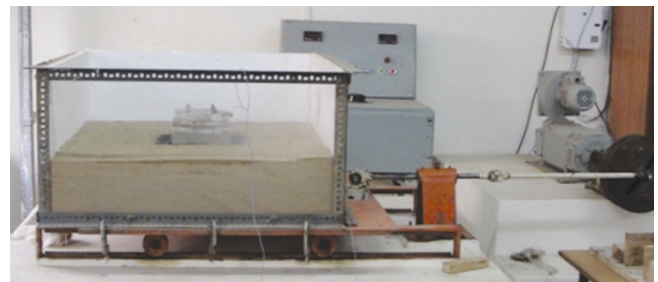
Figure 1. Test set-up.

this study. However, the frequency is scaled by $\lambda^{-0.5}$ and time is scaled by $\lambda^{0.5}$.

A system calibration has been initially done to check the performance of the experimental set-up before starting the work. The objective of the calibration is to verify that the amplification produced by the system is negligible. The loading sequence used for the system calibration consists of 10 sec of horizontal sinusoidal motion with peak acceleration of 0.1 g at 4.65 Hz frequency. No significant amplification of the system is registered during the loading and the system appears to behave linearly throughout the loading history. The vertical vibration of the shaking base plate and the model box is also measured. The magnitude of the vertical vibration (0.0075 g) of the base plate is less compared to the horizontal input motion and cannot significantly affect the test results. The natural frequency of the base plate along with the test container and the soil slope is determined experimentally by subjecting the whole test set-up to motion and then allowing it to shake freely until it stops on its own. The natural frequency of the whole test set-up is around 40 Hz, which is much higher than the predominant frequency of the system. Details of the calibration process are given in Giri and Sengupta[16].

The first series of tests is performed with the model footing placed on top of the sand layer at the middle of the container. The second series of tests is performed with a geo-grid and a geo-textile placed between the model footing and the sand foundation in the test tank. The third series of the tests is performed with the shredded rubber tyre and sand mixture in different proportions as base isolator under the model footing. Before the second and third series of tests, a 20 mm deep square excavation in sand of size 250 mm × 250 mm is constructed. In the second series of tests, the square geo-grid/ geo-textile of 250 mm × 250 mm size is placed at the bottom of the excavation and the excavation is then backfilled with the same sand. The model footing is placed over this backfilled sand after proper compaction. In the third series of tests, the shredded rubber tyre and sand in predetermined proportion (by weight) are mixed thoroughly by hand. The excavation in the sand foundation is then filled with the shredded rubber tyre and sand mixture in three equal layers. Each of the layers is compacted by hand tools to the desired density to avoid undesirable settlements. The model footing is then placed over the shredded tyre and sand mixture. Several proportions of shredded tyre in the shredded rubber tyre-sand mixture have been considered. But only the performance of sand mixed with 50% shredded rubber tyre has been reported here, as it yielded the best result.

The shake table along with the experimental set-up is shaken in the horizontal direction by sinusoidal motion of amplitude 0.15, 0.3, 0.4, 0.6 and 0.8 g. The frequency of motion is varied from test to test to study the effectiveness of the seismic isolators at different frequencies of

motion. The different frequencies considered here are 1.5, 3.5 and 4.5 Hz. For each specified motion, the vertical and horizontal accelerations of the shake table in addition to those on top of the foundation sand layer and on top of the model footing are also recorded. Each motion is continued for at least five cycles to ensure that the system has reached a steady-state condition. A typical input base motion is shown in Figure 2. In all the cases, the results for the first few cycles are only shown for clarity of the presentation.

The performance of sand as a base isolator has been studied for the given base motion mentioned earlier. In this case, the model footing is resting directly on top of 200 mm deep sand layer within the test tank. The sand used in the study is uniform and medium grained sand (Kansai River sand). It is classified as poorly graded sand (SP) according to the Unified Soil Classification System. The specific gravity of the sand is 2.7. The maximum and minimum dry unit weights are 16.6 and 14.1 kN/m³ respectively. In all the tests, the relative density of the sand foundation within the test chamber is maintained at 65%. The shear strength (effective cohesion, c' and effective friction angle, ϕ') of the sand, as obtained from the laboratory direct tests, are given by $c' = 0$ and $\phi' = 36°$.

Figure 3 a shows the transmitted peak accelerations at the top of the footing resting on sand with respect to the peak acceleration of the base motion for different amplitudes of motion (keeping the frequency constant at 3.5 Hz). The figure shows that at and around 0.6 g amplitude of base motion, the sand beneath the model footing starts to dampen the base motion. This is accompanied by a sliding movement of the model footing. Figure 3 b shows the footing response at 1 g amplitude of base motion. The damping effect of the sand in the foundation at this high amplitude of motion can be easily observed from the figure. The maximum amplitude of the footing response reduces to 0.7 g for the 1 g base motion. The relative displacement of the footing is also noticeable at this high amplitude of motion. Figure 3 c shows the relative
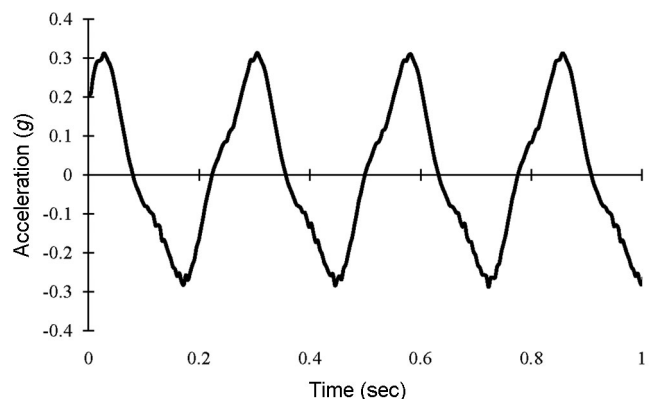
Figure 2. A typical input base motion (amplitude = 0.3 g and frequency = 3.5 Hz).
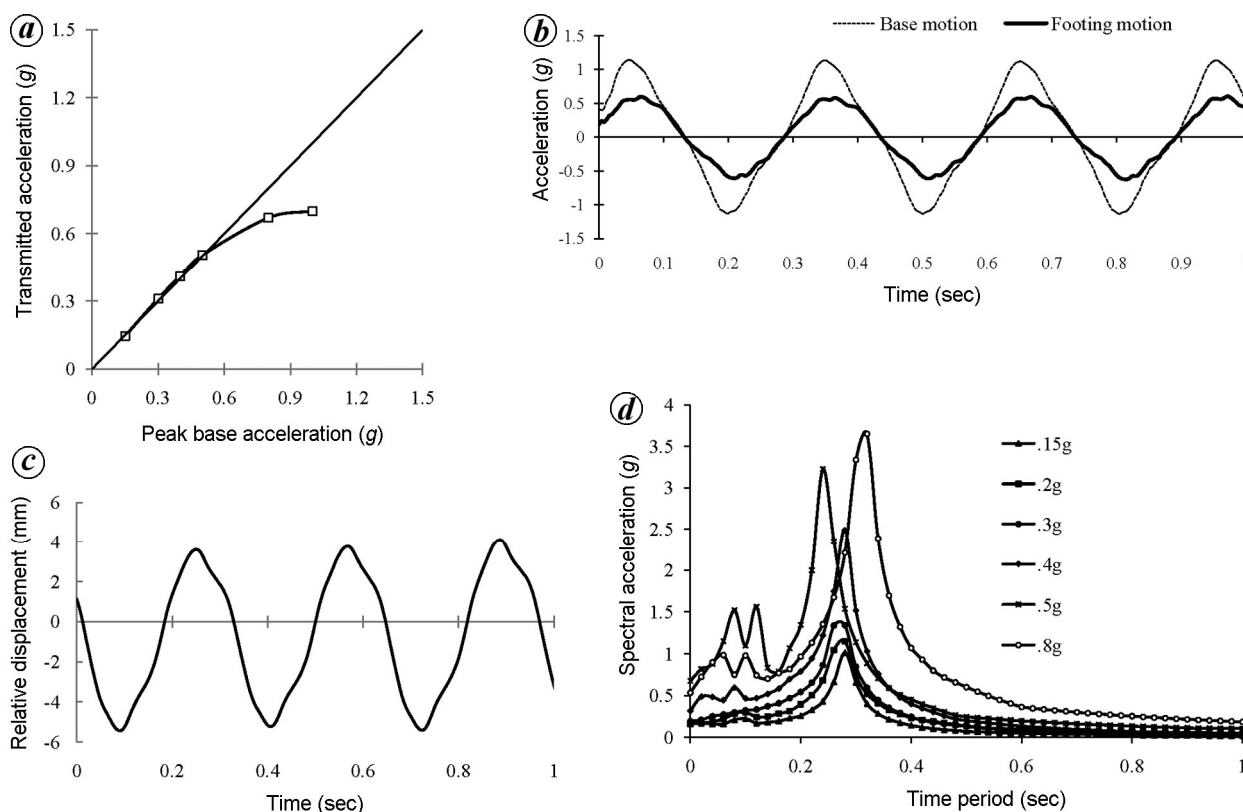
Figure 3. Performance of the footing resting on sand. *a*, Transmitted acceleration at the top of the footing for 0.3 *g* and 3.5 Hz base motion. *b*, Acceleration at the top of the footing for 1 *g* and 3.5 Hz base motion. *c*, Relative displacement of the footing for 1 *g* and 3.5 Hz base motion. *d*, Response of the footing at different amplitudes of motion keeping frequency constant at 3.5 Hz.

displacement of the footing when shaken at 1 *g*. The footing is found to displace back and forth by ± 5.43 mm during the 1 *g* base motion. At the high amplitude of base motion, the relative displacement of the footing over the sand foundation triggers frictional resistance at the interface between the footing and the sand foundation. As the dynamic interface frictional resistance (about 0.6) is exceeded, the footing starts to slip over the sand, which in turn absorbs some of the energy of the base motion and this results in the dampened response of the footing as observed in Figure 3 *b*. Figure 3 *d* shows the response spectra of the model footing resting on the sand at various amplitudes of motion. Note the shifting of the response curve to the right side at high amplitude of motion. This may be due to the slight reorientation (slippage) of the footing on the sand bed at high amplitude of motion. Thus the sand layer in the foundation behaves as an effective base isolator only at high amplitude (above 0.6 *g* in these cases) of base motion.

Consider the case when a geo-grid/geo-textile is placed underneath the model footing and on top of the sand foundation. The geo-grid used in the present study is an extruded polymer mesh made using high-density polyethylene (HDPE) with square openings of size 1.5 mm × 1.5 mm. The mass of the geo-grid is 140 g/m² and its

thickness is 0.28 mm. The ultimate tensile strength is 4 kN/m. The secant modulus of the geo-grid at 5% strain level is 62 kN/m. The geo-textile utilized here is a 200 gsm non-woven material. The ultimate tensile strength of the material is found to be 2.3 MPa. The size of the both geo-grid and geo-textile are 250 mm × 250 mm, that is, 25 mm bigger than the model footing in all directions.

Figure 4 *a* and *b* show the responses of the footing resting on geo-grid and geo-textile respectively, when subjected to base motion at a constant frequency of 3.5 Hz. Figure 4 *a* shows that the geo-grid chosen is actually amplifying the base motion transmitted to the top of the footing. As may be seen from the figure, the peak acceleration at the top of the footing is 0.45 *g* corresponding to base motion of 0.4 *g* at 3.5 Hz frequency. The response of the model footing resting on the geo-textile is marginally better than the footing resting on the geo-grid. As may be seen from Figure 4 *b*, the peak acceleration transmitted to the top of the footing is 0.35 *g* corresponding to the base motion of 0.4 *g*, applied at a frequency of 3.5 Hz.

The shredded rubber tyre used for the study was obtained from a local shop. The shredded rubber tyre is heterogeneous in nature. Each thread has different aspect ratio. The maximum length of a rubber thread is 10 mm

with a diameter of about 1 mm. The heterogeneous nature of the shredded rubber and coarse sand, in fact, helps in reducing the void ratio and achieving a desirable compaction to reduce settlement of the model footing.

Four different proportions (by weight) of shredded rubber tyre – 10%, 20%, 30% and 50% in sand have been utilized in this study as potential low-cost base isolators under the model footing. However, only the results of 50% shredded rubber tyre-sand mixture have been presented here, since this case exhibits the best results under the present scenario. The static shear strengths of the sand and sand mixed with different proportions of shredded rubber tyre were determined in the laboratory using standard direct shear tests. As the percentage of shredded tyre mixture increases, the effective friction angle (ϕ') is found to decrease. The effective cohesion (c') of the mixture is found to increase with increase in the percentage of shredded rubber tyre. The shear strength of the sand only is given by $c' = 0$ and $\phi' = 36°$, while for the sand mixed with 50% (by weight) shredded rubber tyre, the shear strength is given by $c' = 30$ kPa and $\phi' = 30°$. The maximum and minimum dry unit weights are 10.0 and 7.72 kN/m³ respectively. Table 1 summarizes the unit weight and shear strength of the sand and sand mixed with different proportions of shredded rubber tyre.

The laboratory test results show that the unit weight and the effective friction angle decrease with the addition of shredded tyre in the sand. However, the cohesion starts to pick up with increase in the percentage of shredded tyre in the sand. Thus the net bearing capacity, though decreases initially with the addition of shredded tyre, actually increases significantly for 30% and 50% shredded tyre mixture due to increase in cohesion. But as the percentage of shredded tyre in sand increases beyond 50%, the unit weight and shear strength decrease significantly and settlement (punching failure) during the loading becomes an issue. The bearing capacity and the settlement of the model footing at the end of a cyclic test are shown in Table 1. The shear strength results of sand mixed with different proportions of shredded rubber tyre are in agreement with the published results[17–20]. Ahmed[17] found increase in shear strength up to 39% shredded rubber tyre in the sand–rubber tyre mixture. Beyond 39%, he noticed decline in shear strength. The difference in the proportion of rubber tyre in the mixture after which it becomes unstable might be due to the different types of sand used in the study[17].

In all of these cases, a 20 mm deep square excavation in the sand of 250 mm × 250 mm in size is constructed before the tests. This excavation is then filled with the shredded rubber tyre and sand mixture in correct proportion in three equal layers. The model footing is then placed over the shredded tyre and sand mixture (Figure 5) after proper compaction with hand tools. As done for the previous cases, in this case also the whole test set-up is shaken on the shake table for the previously stated sinusoidal motion.

Comparison of the peak acceleration at the top of the model footing resting on sand mixed with 20%, 30% and 50% of shredded rubber tyre and the peak acceleration of the input (measured during the tests) base motion is shown in Figure 6 a as well as in Table 2. It may be seen that the attenuation of the base acceleration is maximum when the proportion of shredded rubber tyre in the sand is 50%. No attenuation of motion is noticed at 0.15 g. However, attenuation of the base motion increases significantly with increase in the magnitude of the base motion for the case of 50% shredded rubber tyre in sand. When the percentage of shredded rubber tyre in the foundation is increased beyond 50%, the footing starts to wobble and becomes unstable.

Figure 6 b shows the response spectra of the footing resting on various percentages of shredded rubber tyre
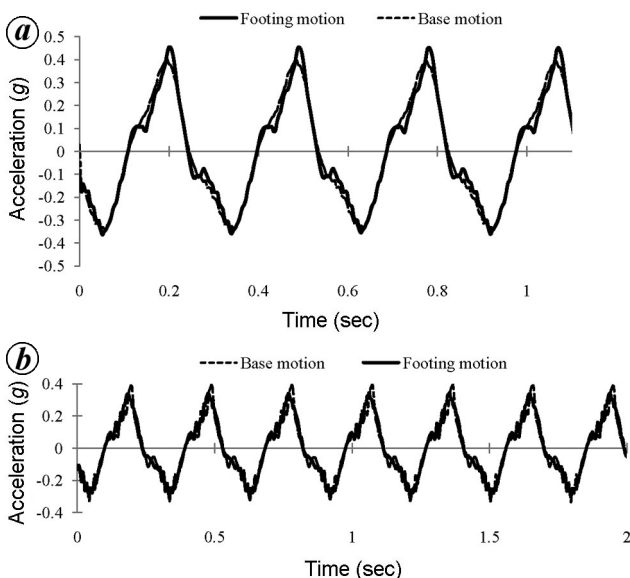
Figure 4. Response of footing resting on top of geo-grid and geo-textile to 0.4 g and 3.5 Hz base motion. *a*, Response of footing resting on top of geo-grid. *b*, Response of footing resting on top of geo-textile.

Figure 5. A view of the model footing (with surcharge load on top) resting on a base isolator consisting of 50% sand and 50% shredded rubber tyre.

Table 1. Material properties, net bearing capacity and settlement of sand and tyre mixtures

Material	Unit weight (kN/m³)	Cohesion c' (kPa)	Friction angle φ' (deg.)	Net bearing capacity* (kPa)	Settlement of foundation block at the end of motion⁺ (mm)
Sand	16.7	0	36	173	0.85
Sand + 20% shredded tyre	14.5	0	34	120	2.38
Sand + 30% shredded tyre	12.0	20	32	1037	3.02
Sand + 50% shredded tyre	10.0	30	30	1235	3.33

*For the model footing. ⁺Differential settlement found to be negligible for all the cases.
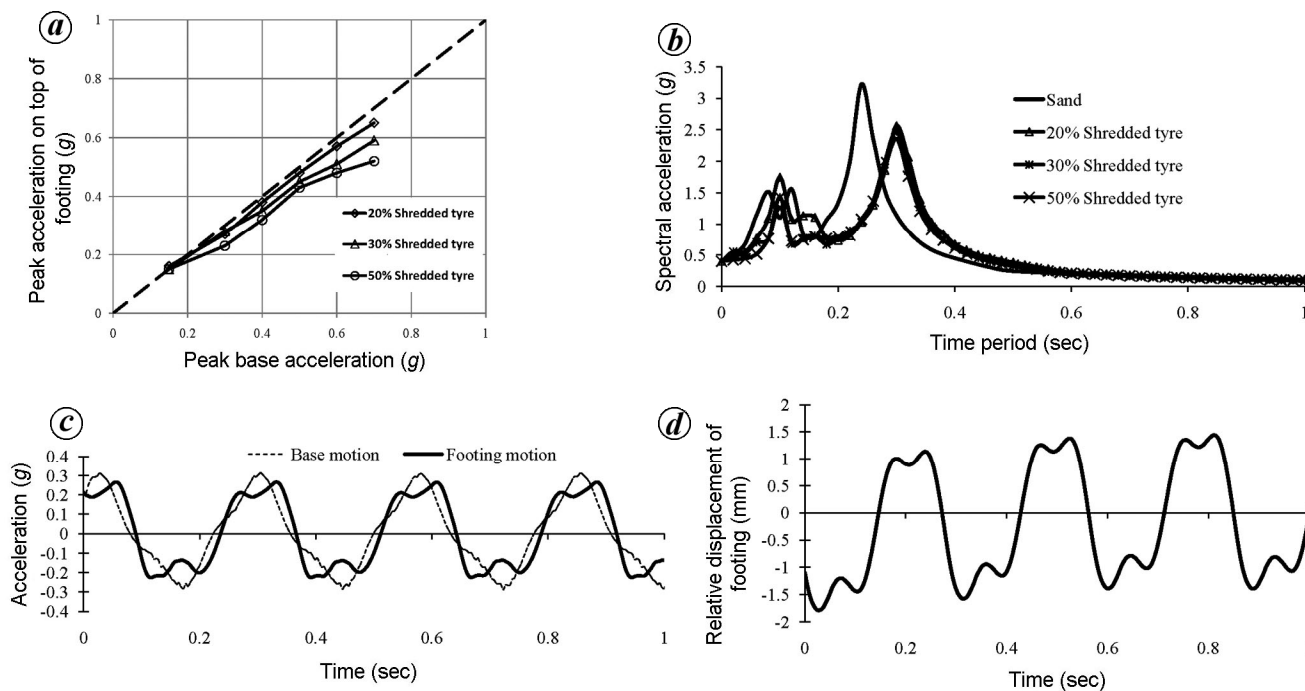
Figure 6. Performance of the model footing resting on sand and 50% shredded rubber tyre. *a*, Comparison of transmitted acceleration at the top of the footing resting on sand and 20%, 30% and 50% shredded rubber tyre for 0.4 *g* and 3.5 Hz base motion. *b*, Response of footing resting on sand and 20%, 30% and 50% shredded rubber tyre for 0.4 *g* and 3.5 Hz base motion. *c*, Comparison of the acceleration on top of the footing resting on sand and 50% shredded rubber tyre with the base motion of 0.3 *g* at 3.5 Hz. *d*, Relative displacement of the model footing resting on sand and 50% shredded rubber tyre for base motion of 0.3 *g* at 3.5 Hz.

and sand and compares them with the response spectra of the footing resting on the sand. The initial peak in the response curves is most probably due to the vibration of the system at low frequency range and it may be ignored. The response curves show increase in damping behaviour due to increase in percentage of shredded rubber tyre in the sand. When compared with the response of the footing resting on sand, a shift in the natural frequency is noticeable (Figure 6 *c*). This might be due to the introduction of a 20 mm thick layer of sand and shredded rubber tyre mixture under the model footing. The relative displacement of the model footing for the case of the footing resting on sand and 50% shredded rubber tyre is found to be about ± 1.8 mm for 0.3 *g* base motion at 3.5 Hz frequency as shown in Figure 6 *d*.

The test results show that, unlike in sand, even at small amplitude of base motion, the response of the model foot-

ing is remarkably less than the base motion. In these cases, the sand rubber mixture dissipated base motion energy through slip deformation, and also some amount of energy is absorbed by the sand rubber mixture which results in dampened response of the footing. The isolating layer consisting of sand mixed with 50% shredded rubber tyre is quite effective in dampening the cyclic base motions. Figure 6 attests to the effectiveness of the sand mixed with 50% shredded rubber tyre as a base isolator for cyclic motions. The test conducted with higher than 50% shredded rubber tyre in sand shows instability even at very small amplitudes of base motion. The model footing with 2 kPa surcharge pressure on top begins to wobble at the initial stage of the test and the test is discontinued. The tests with higher surcharge loads indicate that the stability of the model footing increases with the higher surcharge loads.

Table 2. Attenuation of base motion at different percentages of shredded rubber tyre in sand

Peak base motion (g)	Attenuation of motion at different percentages of shredded rubber tyre in sand		
	20	30	50
0.15	0.15	0.15	0.15
0.3	0.27	0.26	0.23
0.4	0.38	0.35	0.32
0.5	0.48	0.45	0.43
0.6	0.57	0.51	0.48
0.7	0.65	0.59	0.52

The sand in the foundation of the model footing is found to be ineffective as a base isolator at low amplitude (<0.6 g) of base motion. However, at higher amplitude (>0.6 g) of motion, it is quite effective in reducing the motion transmitted to the footing. At 0.8 and 1 g, the acceleration at the top of the model footing shows a remarkable decrease and this is accompanied by back and forth displacement of the footing over the sand foundation. At 1 g of motion, the amplitude of this displacement is observed to be about ± 5.43 mm.

The shake table tests with the model footing resting on a 20 mm layer of sand and shredded rubber tyre show that the proportion of shredded rubber tyre should be 50% (by weight) to yield significant favourable results. When the proportion of the shredded rubber tyre is 50%, the responses of the model footing are found to be significantly less than the motion of the foundation and the shake table. When the percentage of rubber is further increased, the model footing is found to wobble (unstable) at 0.3 g motion.

All the tests are conducted in a rigid container mounted on a uniaxial shake table. The proximity of the rigid boundaries definitely has some effect on the footing responses, but attempts have been made to minimize them by fixing 30 mm thick thermocol sheets at the inner boundaries of the container to minimize the reflection of the waves.

A base isolating system can be effective in two ways: (i) by reducing the input motion that the structure is subjected to and (ii) by shifting the predominent frequency of the structure from that of its base motion, so that resonance of frequency cannot be achieved. This communication only addresses the base isolation by dampening of the input motion. Since all the input motions of the shake table are sinusoidal with a given frequency, the shifting of the frequency of the model footing during a test could not be studied. This important aspect of the base isolation system will be investigated in the next phase of the study.

The results presented here are based on small-scale model study in the laboratory. More detailed study on full-scale models is necessary before it can be implemented in real-life situations.

1. Soong, T. T., State-of-the-art review, active structural control in civil engineering. *Eng. Struct.*, 1988, **10**, 74–84.
2. Jangid, R. S. and Datta, T. K., Seismic behavior of base-isolated buildings: a state-of-the-art review. *Proc. ICE: Struct. Build.*, 1995, **110**, 186–203.
3. Nagarajaiah, S., Semi-active control of structures. In Proceedings of Structural Congress XV, ASCE, Portland, Oregon, USA, 1997, pp. 1574–1578.
4. Ehrgott, R. C. and Masri, S. F., Structural control applications of an electro-rheological device. In Proceedings of International Workshop on Structure Control, University of Southern California, Los Angeles, USA, 1994, pp. 115–129.
5. Kelly, J. M., Base isolation: linear theory and design. *Earthquake Spectra*, 1990, **6**, 234–244.
6. Kelly, J. M., *Earthquake-resistant Design with Rubber*, Springer, New York, 1996, 2nd edn.
7. Paulay, T. and Priestley, M. J. N., *Seismic Design of Reinforced Concrete and Masonry Buildings*, Wiley, New York, 1992.
8. Qamaruddin, M. and Ahmad, S., Seismic response of pure friction base isolated masonry building with restricted base sliding. *J. Eng. Res.*, 2007, **4**, 82–94.
9. Qamaruddin, M., Arya, A. S. and Chandra, B., Seismic response of brick buildings with sliding substructure. *J. Struct. Eng.*, 1986, **122**, 558–572.
10. Feng, M. Q., Shinozuka, M. and Fuji, S., Friction-controllable sliding isolation system. *J. Eng. Mech.*, 1993, **119**, 1845–1864.
11. Yegian, M. K. and Kadakal, U., Foundation isolation for seismic protection using a smooth synthetic liner. *J. Geotech. Geo-environ. Eng.*, ASCE, 2004, **130**, 1121–1130.
12. Yegian, M. K. and Catan, M., Soil isolation for seismic protection using a smooth synthetic liner. *J. Geotech. Geo-environ. Eng.*, ASCE, 2004, **130**, 1131–1139.
13. Edil, T. B. and Bosscher, P. J., Engineering properties of tyre chips and soil mixtures. *Geotech. Testing J.*, ASTM, 1994, **17**, 453–464.
14. Gray, D.-H. and Ohashi, H., Mechanics of fiber reinforcement in sand. *J. Geotech. Eng.*, ASCE, 1983, **112**, 804–820.
15. Tsang, H. H., Seismic isolation by rubber–soil mixtures for developing countries. *Earthquake Eng. Struct. Dyn.*, 2008, **37**, 283–303.
16. Giri, D. and Sengupta, A., Dynamic behavior of small scale nailed soil slopes. *Geotech. Geol. Eng.*, 2009, **27**, 687–698.
17. Ahmed, I., Laboratory study on properties of rubber–soils. In Joint Highway Research Project Report No. 3-36-50L, Indiana Department of Transportation and Department of Civil Engineering, Purdue University, Indiana, USA, 1993.
18. Shariatmadari, N., Karimpour-Ford, M. and Roustazadeh, M., Waste tyre shreds as soil reinforcement. In International Conference on Non-Conventional Materials and Technologies: Ecological Materials and Technologies for Sustainable Building, Maceio, Alaqoas, Brazil, 2007.
19. Youwai, S. and Bergado, D. T., Strength and deformation characteristics of shredded rubber tyre–sand mixture. *Can. Geotech. J.*, 2003, **40**, 254–264.
20. Balachowski, L. and Gotteland, P., Characteristics of tyre chips–sand mixtures from triaxial tests. *Arch. Hydro–Eng. Environ. Mech.*, 2007, **54**, 25–36.